Measurements and assessment of $^{12}C(d,p\gamma)^{13}C$ reaction cross sections in the deuteron energy range 740–2000 keV for analytical applications

L. Csedreki[*1)], I. Uzonyi[1)], G.Á. Szíki[2)], Z. Szikszai[1)], Gy. Gyürky[1)], Á.Z. Kiss[1)]

[1)]Institute for Nuclear Research, Hungarian Academy of Sciences, MTA Atomki

H-4001 Debrecen, P.O. Box 51, Hungary

[2)]Department of Basic Technical Studies, Faculty of Engineering, University of Debrecen,

H-4028 Debrecen, Ótemető u. 2-4, Hungary

[*)] Corresponding author. Tel.: +36 52 509200; fax: +36 52 416181.

E-mail address: csedreki@atomki.mta.hu

Abstract

The total cross sections of the $^{12}C(d,p\gamma_1)^{13}C$ ($E\gamma$ = 3089 keV) , $^{12}C(d,p\gamma_2)^{13}C$ ($E\gamma$ = 3684 keV) and $^{12}C(d,p\gamma_3)^{13}C$ ($E\gamma$ = 3854 keV) reactions, as well as differential cross sections for (d,p_o), (d,p_1) reactions and (d,d_0) elastic scattering were determined in the 740-2000 keV deuteron energy range using a self-supporting natural carbon foil and detecting the gamma-rays and particles simultaneously. In order to test the validity of the measured gamma-ray producing cross sections, benchmark experiments were performed using kapton foils with two different thicknesses. Both the obtained gamma- and particle production cross section results were compared with data existing in literature, and in the case of (d,p_o) the experimental differential cross-section data were compared also with the theoretical evaluated values.

PACS: 29.30.Kv; 82.80.Ej; 81.70.-q; 25.45.-z
Keywords: DIGE; Cross sections for gamma-ray and particles; E_d = 0.74–2 MeV; ^{12}C+d reactions

1. Introduction

Particle Induced Gamma-ray Emission (PIGE) spectroscopy is an excellent tool to measure the concentration of light elements such as carbon. The $^{12}C(d,p\gamma)^{13}C$ nuclear reaction has already been applied in materials science for the determination of carbon in steels [1] and to characterize high purity, high performance thin films produced by metal-organic chemical vapour deposition (MOCVD) technique. Regarding the characterization of thin films, the advantage of the PIGE method is its sensitivity; it is capable to detect rather low carbon concentrations and C/O ratios in the presence of different kind of substrates [2, 3].

Gamma-ray production yields in deuteron induced nuclear reactions (d-PIGE) for thick targets were published in [4] for several deuteron energies; however, for precise quantitative analysis, the cross section of the reaction as a function of deuteron energy is needed. To our best knowledge, the following cross section measurements exist in literature: Tryti et al. [5, 6] studied primarily the behaviour of this reaction in terms of nuclear physics, while the aim of the later measurements [7, 8] was the application of the resulted cross sections for elemental analysis (archaeometry and geology, respectively). The comparison of the published cross sections revealed rather large discrepancies.

The aim of this work is to determine reliable cross section data for the $^{12}C(d,p\gamma)^{13}C$ nuclear reaction by carrying out the measurement of gamma-ray producing cross sections with the detection of gamma- and particle yields simultaneously. In this paper we report on the measurements of the total $^{12}C(d,p\gamma_1)^{13}C$ ($E\gamma$ = 3089 keV), $^{12}C(d,p\gamma_2)^{13}C$ ($E\gamma$ = 3684 keV) and $^{12}C(d,p\gamma_3)^{13}C$ ($E\gamma$ = 3854 keV) reaction cross sections, as well as differential cross sections for (d,p_o), (d,p_1) reactions and (d,d_0) elastic scattering, respectively. In order to test the measured cross sections in relation to the thick target yields, benchmark experiments were performed. Both the obtained gamma-ray and particle production cross section results were compared with data existing in literature, and in the case of (d,p_o) it was a possibility to compare the experimental differential cross section data with the theoretical evaluated values published by Abriola et al [9] recently.

The present work is part of a Coordinated Research Project organized by IAEA [10, 11] and the experimental results will be incorporated into IBANDL (Ion Beam Analysis Nuclear Data Library, www-nds.iaea.org/ibandl/).

2. Experimental

The measurements were carried out at the 5 MV Van de Graaff accelerator of Atomki. The energy calibration of the accelerator for protons was performed with the 992 keV resonance of the $^{27}Al(p,\gamma)^{28}Si$ reaction. Besides the calibration with protons, the 1449±1.5 keV resonance [12] of the $^{12}C(d,p\gamma)^{13}C$ reaction was also used to check the energy calibration.

The experimental set-up consisted of a target chamber with a long Faraday cup, a coaxial type HPGe detector of 170 cm^3 volume positioned at an angle of 55° relative to the beam direction at a distance of 9.5 cm from the target, and an ion implanted Si detector with 500 μm active depth and 13 keV energy resolution was placed at an angle of 135° relative to the beam direction at a distance of 4.15 cm from the target. A copper collimator with a hole diameter of 3 mm was used in front of the Si detector. The determination of the solid angle of the Si detector was done with a Th(B+C) radioactive source with a well known activity. The solid angle was found to be 4.11±0.10 msr. The detailed description of the experimental set up including the absolute efficiency determination of the HPGe gamma detector is presented elsewhere [13].

The target was a self-supporting natural carbon foil (thickness: $1.9*10^{18}$ atom/cm^2) with an evaporated palladium layer on its back surface (thickness: $2.7*10^{17}$ atom/cm^2). The number of target nuclides was determined with α-RBS technique directly before and after the cross section measurements and under the same experimental conditions using the SIMNRA program [14]. The applied α-energy was 1.5 MeV. At this incident energy the backscattering of alpha particles can be considered as pure Rutherford on both C and Pd [15]. In order to check the stability of the target, and also the possible build-up of carbon on its surface, the thin target gamma-ray and proton yields were re-measured in several energy points directly after finishing the actual yield measurements. Comparing the α-RBS thickness data that was obtained before and after the yield measurements, and also on the basis of the gamma-ray and proton yield re-measurements, we can conclude that the damage of the target and the carbon build-up on its surface were below 5%, so within the uncertainties; in addition, the overall sum of these deviations was close to zero. Figs. 1 and 2 show the gamma-ray and particle spectra of the target measured simultaneously at 2.0 MeV deuteron energy. The interaction of the beam with the carbon contaminants of the experimental set-up has to be taken into consideration because it also gives a contribution to the measured gamma-ray yields thus decreases the accuracy of the calculated cross sections. Our test measurements carried out with an empty target holder at different gamma energies showed that this contribution is (3±1)%, thus we corrected our final results with this value.

Gamma-ray yields for the 3089, 3684 and 3854 keV gamma-lines of the $^{12}C(d,p\gamma)^{13}C$ reaction and $^{12}C(d,p_0)^{13}C$, $^{12}C(d,p_1)^{13}C$, $^{nat}C(d,d_0)^{nat}C$ reaction particle yields were measured. The measurements were performed starting from 2000 keV deuteron energy and descending to 740 keV with 2-20 keV steps depending on the structure of the excitation function, and was repeated at certain deuteron energies several times. Typical beam current and collected charge were 25 nA and 7 μC, respectively. The simultaneous collection of gamma-ray and particle spectra as it was proposed in reference [11] has the advantage of the independent determination of the beam charge with the RBS monitoring of the Pd layer, which helps to avoid systematic and stochastic uncertainties of charge integration.

3. Cross section calculations and discussion of the results

3.1 Gamma-ray production cross sections

The total gamma-ray production cross section was determined according to the following equation:

$$\sigma_\gamma(E_0,\theta) = \frac{Y_\gamma(E_0,\theta)}{N_p N_{t-C} \varepsilon_{abs}(E_\gamma)} \qquad (1)$$

where $Y_\gamma(E_0,\theta)$ is the measured γ-ray yield (i.e. the net area of the γ-ray peak) at deuteron energy E_0 and γ-ray detection angle θ, N_p is the number of incident projectiles, $N_{t\text{-}C}$ is the number of carbon nuclei per square centimeter and $\varepsilon_{abs}(E_\gamma)$ is the absolute detection efficiency of the HPGe detector at the corresponding gamma-ray energy [10]. This formula is valid only if the cross section is varying only little within the target thickness, which requirement is satisfied approximately for the entire energy range except at resonant energies. Therefore, the calculated and presented gamma-ray production cross section values are considered as averaged ones for the finite thickness target.

To avoid the errors stemming from the direct measurement of incident charge, we calculated the number of incident projectiles N_p from the following equation:

$$N_p = \frac{Y_s(E_0,\beta)}{\frac{d\sigma_{Ruth}(E_0,\beta)}{d\Omega} * \Omega \varepsilon N_{t-Pd}} \qquad (2)$$

where $Y_s(E_0,\beta)$ is the measured scattered particle yield for the palladium layer on the target (i.e. the net area of the scattered projectile peak) measured at deuteron energy E_0 and particle detection angle β, $d\sigma_{Ruth}(E_0,\beta)/d\Omega$ is the Rutherford cross section for palladium at deuteron energy E_0 and particle detection angle β and $N_{t\text{-}Pd}$ is the number of palladium nuclei per square centimeter [10].

With this method, we had to ascertain the target nuclide numbers with high precision for both components, and determine the parameters of the experimental system, the solid angle of the particle detector and the absolute efficiency of the HPGe detector. In the calculation of the elastic backscattering cross section for palladium, the changes in the energy of deuterons while moving through the carbon layer had to be taken into account, too.

In order to keep statistical uncertainty low, in the case of the $^{12}C(d,p\gamma)^{13}C$ reaction for the $E\gamma_1$=3089 keV gamma-line, which was the most important for us because of its analytical importance, we aimed to reach a peak area with 10000 counts. After the evaluation we obtained 1-2% error for the net peak counts. For the gamma production reactions of $E\gamma_2$= 3684 keV, $E\gamma_3$= 3854 keV energies, the error was 2-42% because of the lower intensities. In the evaluation process, dead time (<1%) correction was applied.

Based on α-RBS measurements, the overall uncertainty of $N_{t\text{-}C}$ and $N_{t\text{-}Pd}$ was found to be 3% (measurements on a SiPd standard series and repeated measurements of the sample were taken into account). The error of the solid-angle (Ω) determination of the particle detector was 2.5%, the uncertainty of the activity determination of the Th(B+C) source included.

Concerning the Rutherford backscattering calculation of the palladium layer, an error of 2% is estimated, due to the uncertainties of the angle determination and energy loss through the carbon layer.

The uncertainty of the absolute efficiency (ε_{abs}) of the HPGe detector is 2% at 3089 keV and 3% at 3684 and 3854 keV, based on the measured efficiency curve.

The total errors obtained from the quadratic sum of the partial uncertainties are below 6%, in the case of the $^{12}C(d,p\gamma_1)^{13}C$ reaction while it varied between 5-38% and 6-43% in the cases of $^{12}C(d,p\gamma_2)^{13}C$ and $^{12}C(d,p\gamma_3)^{13}C$ reactions, respectively.

The obtained gamma-ray production cross section for the $E\gamma_1$=3089 keV line as a function of the bombarding deuteron energy and the result of measurement from 0.74 to 2.0 MeV is presented in Fig. 3. The threshold energy for this gamma transition is 428 keV, not much below the experimentally studied energy range. The present results can be compared with three previous works [5-7] while the work of [8] is excluded from the comparison, because it contains data only in a limited deuteron energy interval (1.4-1.9 MeV). A summary of the experimental details of the three previous works and the present one is presented in Table 1. As it is seen from Table 1. Tryti et al. gave their cross section values in arbitrary unit in their first paper [5]. However, the experimental conditions of ref. [5,6] works were practically the same, and the deuteron energy dependence of total cross sections given by [6] overlaps in a large interval with the cross section values of ref. [5], thus it was possible to normalize the two curves and to give the cross sections in the unit of mbarn in the whole energy range in Fig. 3. Comparing the values with the present results, the curves of Tryti are only about 7% below the present one up to about 1500 keV. At higher energies the deviation of Tryti's data is increasing gradually and exceeds the 25%. The excitation function of Papillon et al. [7] is shifted towards lower energy values. This discrepancy can be most easily observed in the position of the 1449.5 keV resonance. The resonance appears 36 keV below the literature value. The authors certainly had a wrong accelerator energy calibration. (The other well defined resonance at 2494 keV [12] is shifted down only with 14 keV, which means that the wrong energy calibration can not easily be corrected.) Despite of the energy shift, these cross section data agrees with the present values within ± 5% (considering the "peaks" and "valleys" in the two curves); however, above 1500 keV deuteron energy Papillon's data are 8 -10% below the present ones.

Figures 4 and 5 show the gamma-ray production cross sections belonging to the 3684 and 3854 keV gamma-lines, including also the literature data. The threshold energies for these two reactions are 1122 and 1321 keV, respectively. In the intensity of the peak of the excitation curve of the 3684 keV gamma-line there is a deviation 6% and 17% between the present values and that of Papillon at al.[7] and Tryti et al.[5,6], respectively, although these do not exceed significantly the experimental errors of the three measurements. While the 3089 keV excited state in ^{14}N has spin ½ and therefore the emitted gamma rays are isotropic, the 3684 keV and 3854 keV excited states of ^{14}N have spin values -3/2 and +5/2 , respectively, thus the emission lines are not isotropic, thus strictly speaking the cross sections presented in Figs. 4 and 5 are not total cross sections. We performed similar gamma-ray angular distribution

measurements as it was described in our previous paper [13], and the results showed, that the anisotropy was below 6% between 30-135 degree with respect to the beam direction in the case of 3684 keV gamma-line at 1727 keV deuteron energy, which is within the experimental error quoted above. We note that this small and negligible anisotropy is valid for the energy range around the measured point only and might be different at other energies.

Benchmarking measurements

Cross section data intended for analytical purposes, either measured or evaluated, must be verified through benchmarking experiments on well characterized targets [16].

To test the validity of our cross section data's energy dependence, we carried out measurements on 125 μm (infinitely thick) and 16 μm (580 keV thickness at E_d=2000 keV) intermediate thick kapton ($(C_{22}H_{10}N_20_5)_n$) foils at 2000 keV deuteron energy and calculated the mass fraction of carbon in them applying the following formula, which was derived from equation 1 by integration:

$$f_m = \frac{Y_\gamma(E_0,\theta)}{\varepsilon_{abs}(E_\gamma) f_i N_p N_{Av} A^{-1} \int_{E_i}^{E_0} \frac{\sigma(E,\theta)}{S(E)} dE} \qquad (3)$$

where f_m is the mass fraction of the analysed element, $Y_\gamma(E_0,\theta)$ is the measured gamma-ray yield on the thick or intermediate thick target (i.e. the area of the gamma-ray peak) at projectile energy E_0 and gamma-ray detection angle θ, N_p is the number of incident projectiles, $\varepsilon_{abs}(E_\gamma)$ is the absolute efficiency of the gamma-ray detector correspondent to the E_γ energy gamma-ray line, f_i is the abundance of the isotope producing the gamma-radiation, N_{Av} is the Avogrado number, A is the atomic mass of the analysed element, E_1 is the energy of the projectile after transmitting the target (for infinite thick targets E_1=0), σ(E,θ) is the absolute gamma-ray production cross section at projectile energy E and gamma-ray detection angle θ, and S(E) is the stopping power of the projectile in the target in energy per areal mass unit. The ∫[E_1, E_0] σ(E,θ)/S(E) dE integral was calculated numerically dividing the [E_1, E_0] energy range into 2-20 keV long intervals.

The integration procedure contains two kinds of inaccuracies. One is originating from the uncertainties of the measured cross sections, the other one is that there is no experimental cross section data between the threshold and 740 keV. Supposing a constant cross section in this energy range, its contribution to the total thick target yield remains below 5% and therefore can be neglected. The value of E_1 for the 16μm thick kapton foil is 1420 keV. These results are shown in Table 2. The discrepancies are lower than 4% between the calculated and nominal mass fraction of carbon, which value remains under the average uncertainty of cross section data. Thus the results of benchmarking process support our cross section reliability exceedingly.

3.2 Particle cross sections

In order to increase the validity of our gamma-ray production cross sections, we compared our particle production cross section data with the ones in literature.

The particle production cross section can be written as:

$$\frac{d\sigma(E_0,\beta)}{d\Omega} = \frac{Y(E_0,\beta)}{N_p N_{t-C} \Omega \varepsilon} \qquad (4)$$

where $d\sigma(E_0,\beta)/d\Omega$ is the differential particle production cross section at deuteron energy E_0 and particle detection angle β, $Y(E_0,\beta)$ is the measured particle yield (i.e. the net area of the particle peak) measured at deuteron energy E_0 and particle detection angle β, ε is the intrinsic efficiency of the particle detector (usually ~100%), Ω is the solid angle of particle detection (assumed to be small), N_p is the number of incident ions calculated from equation (2) and $N_{t\text{-}C}$ is the number of carbon nuclei per square centimeter. Concerning the particle reactions, the errors of the counting statistics were between 1-7%.

The characteristic final error of our particle production cross section data is 5%

The comparison with literature data is the most straightforward in the case of the $^{12}C(d,p_0)^{13}C$ reaction due to the same applied detection angle and the high accuracy and theoretically well established nature of literature data [17]. Figure 6. shows the particle production cross section data measured at the angle of 135^o by [18-21] together with the data measured in the present work. We obtained the best similarity with the data obtained by Carvalho et al. and Kokkoris et al. The deviation from these data is within the data uncertainties at low energy. Between 1760-2000 keV our data are below the above mentioned ones by on average 18% and 29%, respectively.

The comparison with previous gamma and particle cross section measurements show that the agreement with the present values is rather good regarding the quoted accuracy. Our gamma results are somewhat above, while particle results are slightly below previous measurements, no systematic deviations occur, which indicates that the N_p values present in both calculations (eq. 1 and 4.) were well measured.

An important outcome of the present work was that the experimental results at 135^o led to a fine-tuning of the parameters involved in the evaluated curve presented in [9], which is based on DWBA (Distorted Wave Born Approximation) and R-matrix calculations, especially for deuteron beam energies above 1.7 MeV [22]. The new evaluated results are available to the scientific community via the online calculator SigmaCalc 2.0 [17].

Still, according to the calculation, the position of the 1449 keV resonance is somewhat shifted to lower energy. We note that this statement agrees with a work in progress [23] where the large number of gamma and particle cross section results available now make it possible to re-determine the position of the above mentioned narrow resonance around 1449 keV.

As a by-product of this work the $^{12}C(d,p_1)^{13}C$ reaction and the $^{nat}C(d,d_0)^{nat}C$ elastic cross section was also determined. Figure 7 shows the particle production cross section data concerning the $^{12}C(d,p_1)^{13}C$ reaction including the literature data. In the literature, we have found a limited number of data sets close to 135° detection angle. Poore et al. [24] carried out their measurements at 136.1°, but only for a few energy points. Comparing our results with these data, the agreement is satisfactory. Kokkoris et al. published data for 145° [25]. Some

deviation can be observed in the 1570-1850 keV energy range, probably caused by the different angle of detection. Figure 8. shows the comparison of the elastic scattering cross section data of the $^{nat}C(d,d_0)^{nat}C$ reaction, based on the present work (135°), with Kokkoris et al. [26] (145°) and with Jeronymo et al. [27] (143.5°), as no data for the 135 degree is found in the literature. The characteristic final error of our elastic scattering production cross section data is 5%. In the case of Jeronimo's data the cross section data were given in arbitrary unit only. Therefore, a scaling factor of 195 was applied to this data set in order to have the best agreement with the absolute value of the cross section obtained in the present work and by Kokkoris et al. Although the measurements were performed at different angles, the obtained cross section data are still comparable.

4. Summary

Our main goal was the determination of the gamma-ray production cross sections for the 3089 keV gamma line because of its analytical importance. In addition to these measurements new data on $^{12}C(d,p\gamma_2)^{13}C$ ($E\gamma$ = 3684 keV) γ-ray producing cross sections were obtained and the results were compared with earlier published data. The similarities and deviations were assessed. These assessments revealed the possible uncertainties of earlier cross section measurements and contribute to the determination of final excitation functions of $^{12}C(d,p\gamma)^{13}C$ reactions. The results of the benchmarking experiment and the obtained cross sections of the $^{12}C(d,p_0)^{13}C$ reaction verify the accuracy of experimental parameters and therefore increases the reliability of the measured gamma-ray production cross sections. As a by-product we produced new differential cross section data at 135^o in the cases of $^{12}C(d,p_1)^{13}C$ and $^{nat}C(d,d_0)^{nat}C$ reactions.

Acknowledgements

The support of the IAEA Coordinated Research Project "Reference Database for Particle-Induced Gamma-ray Emission (PIGE) Spectroscopy" (Contract No. 16967/R1) is acknowledged.

References

[1] A. Ene, I. V. Popescu, T. Badica, Journal of Optoelectronics and Advanced Materials 8 (2006) 222-224.

[2] M. Banerjee, N. B. Srinivasan, H. Zhu, S. Ja Kim, Ke Xu, M. Winter, H-W. Becker, D. Rogalla, T. de los Arcos, D. Bekermann, D. Barreca, R. A. Fischer, and A. Devi, Crystal Growth Design, 12 (2012) 5079−5089.

[3] Daniela Bekermann, Arne Ludwig, Teodor Toader, Chiara Maccato, Davide Barreca, Alberto Gasparotto, Claudia Bock, Andreas D. Wieck, Ulrich Kunze, Eugenio Tandello, Roland A. Fischer, and Anjana Devi, Chemical Vapor Deposition, 17, (2011) 155-161.

[4] Z. Elekes, Á.Z. Kiss, I. Biron, T. Calligaro, J. Salomon, Nuclear Instruments and Methods in Physics Research B 168 (2000) 305-320.

[5] S. Tryti, T. Holtebekk and J. Rekstad, Nuclear Physics A 201 (1973) 135 -144,

[6] S. Tryti, T. Holtebekk and F. Ugletveit, Nuclear Physics A 251 (1975) 206 -224,

[7] F. Papillon, P. Walter, Nuclear Instruments and Methods in Physics Research B 132 (1997) 468 – 480.

[8] Z. Elekes, Gy. Szöőr, Á.Z. Kiss, P. Rózsa, A. Simon, I. Uzonyi, J. Simulák, Nuclear Instruments and Methods in Physics Research B 190 (2002) 291–295.

[9] D. Abriola, A.F. Gurbich, M. Kokkoris, Nuclear Instruments and Methods in Physics Research B 301 (2013) 41–46.

[10] D. Abriola, P. Dimitriou and A. Pedro de Jesus, Summary Report 2nd Research Coordination Meeting Development of a Reference Database for Particle-Induced Gamma-ray Emission (PIGE) Spectroscopy, IAEA Headquarters, Vienna, Austria, 8-12 October 2012, INDC(NDS)-0625.

[11] A.P. Jesus et al., Interlaboratory excercise for PIGE cross-section measurements, submitted to Nuclear Instruments and Methods in Physics Research B.

[12] F. Ajzenberg-Selove. Nuclear Physics A523 (1991) 1.

[13] L. Csedreki, I. Uzonyi, Z. Szikszai, Gy. Gyürky, G.Á. Szíki, Á.Z. Kiss, submitted to Nuclear Instruments Methods in Physics Research B

[14] M. Mayer, Technical Report IPP 9/113, Max-Plank Institute für Plasmaphysik, Garching, Germany, 1997.

[15] M. Bozoian, M. Hubbard, and M. Natasi, Nuclear Instruments and Methods in Physics Research B51, (1990) 311-319.

[16] D. Abriola, N.P. Barradas, I. Bogdanović-Radović, M. Chiari, A.F. Gurbich, C. Jeynes, M. Kokkoris, M. Mayer, A.R. Ramos, L. Shi, I. Vickridge, Nuclear Instruments and Methods in Physics Research B 269 (2011) 2972–2978.

[17] SigmaCalc 2.0 online calculator (data retrieved from the IBANDL database, http://www-nds.iaea.org/ibandl/).

[18] G. Debras, G. Deconninck, J. RadioAnal. Chem. 38 (1977) 193–204 (data retrieved from the IBANDL database, http://www-nds.iaea.org/ibandl/).

[19] R. A. Jarjis, Int. Rep., U. of Manchester (1979) (data retrieved from the IBANDL database, http://www-nds.iaea.org/ibandl/).

[20] M. Kokkoris, P. Misaelides, S. Kossionides, Ch. Zarkadas, A. Lagoyannis, R.Vlastou, C.T. Papadopoulos, A. Kontos, Nucl. Instr. Meth.B 249 (2006) 77–80 (data retrieved from the IBANDL database, http://www-nds.iaea.org/ibandl/).

[21] J.A.R. Pacheco de Carvalho, A.D. Reis, Nuclear Instruments and Methods in Physics Research B 266 (2008) 2263–2267 (data retrieved from the IBANDL database, http://www-nds.iaea.org/ibandl/).

[22] M. Kokkoris, private communication.

[23] L. Csedreki, G. Á. Sziki, H. Czédli, submitted to Acta Physica Polonica.

[24] R. V. Poore, P. E. Shearin, D. R. Tilley and R. M. Williamson, Nuclear Physics A92 (1967) 97-122. (data retrieved from the IBANDL database, http://www-nds.iaea.org/ibandl/).

[25] M. Kokkoris , P. Misaelides, A. Kontos , A. Lagoyannis , S. Harissopulos, R. Vlastou, C.T. Papadopoulos, Nuclear Instruments and Methods in Physics Research B 254 (2007) 10–16 (data retrieved from the IBANDL database, http://www-nds.iaea.org/ibandl/).

[26] M.Kokkoris P. Misailides, S. Kossionides, A. Lagoyannis, Ch. Zarkadas, R. Vlastou, C.T. Papadopoulos, A. Kontos, Nuclear Instruments and Methods in Physics Research B249 (2006) 81-84 (data retrieved from the IBANDL database, http://www-nds.iaea.org/ibandl/).

[27] J. M.F. Jeronymo, G.S. Mani, F. Picard and A. Sadeghi, Nuclear Physics 43 (1963) 417-423 (data retrieved from the IBANDL database, http://www-nds.iaea.org/ibandl/).

Figure captions

Fig. 1. and 2. Gamma-ray and particle spectrum of the C-Pd target at 2.0 MeV deuteron energy. (The low energy background is due to the scattering from the wall of the chamber, the peak at channel no. 750 is regarded as electronic noise.)

Fig. 3. Gamma-ray production cross section for the 3089 keV gamma-line as a function with deuteron energy.

Table 1. Experimental details of the present and previous measurements

Fig. 4. Gamma-ray production cross section for the 3684 keV gamma-line as a function with deuteron energy.

Fig. 5. Gamma-ray production cross section for the 3854 keV gamma-line as a function with deuteron energy.

Table 2. Results of the benchmarking process

Fig. 6. Present particle production cross section data for the $^{12}C(d,p_0)^{13}C$ reaction measured at 135^0 compared with experimental data from the literature and the theoretical excitation function based on DWBA (Distorted Wave Born Approximation) and R-matrix calculations [22].

Fig. 7. Particle production cross section data for the $^{12}C(d,p_1)^{13}C$ reaction

Fig. 8. Elastic scattering cross section data of the $^{nat}C(d,d_0)^{nat}C$ reaction

Fig. 1.

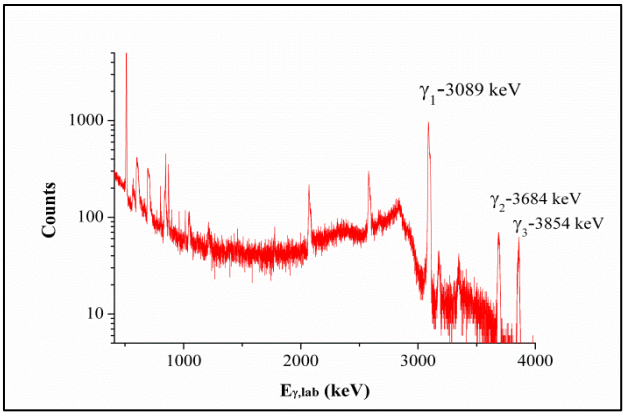

Fig. 2.

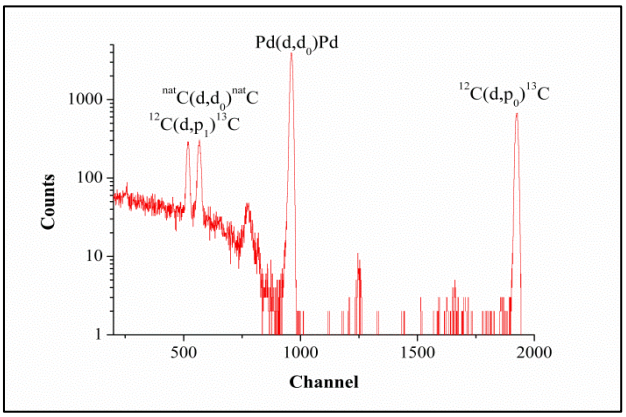

Fig. 3.

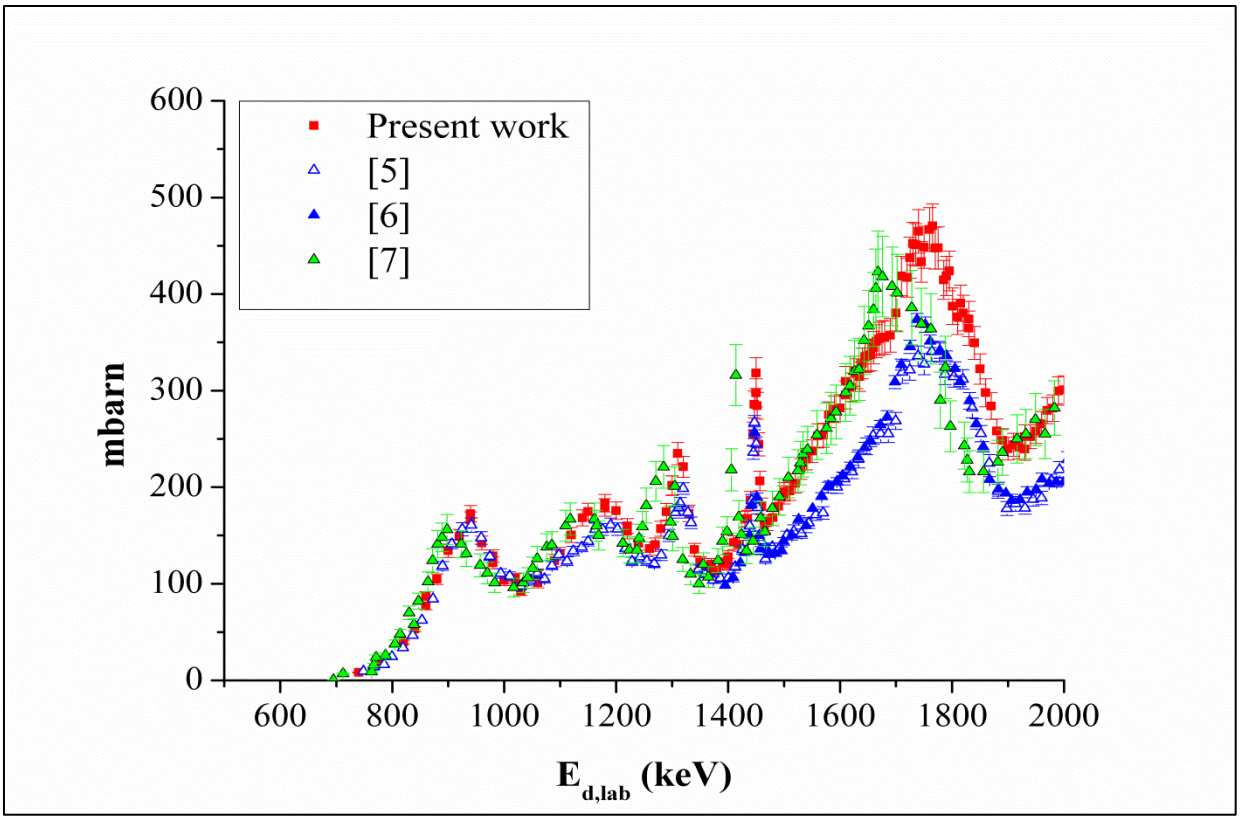
Present work
[5]
[6]
[7]
mbarn
0
100
200
300
400
500
600
600
800
1000
1200
1400
1600
1800
2000
E d,lab (keV)

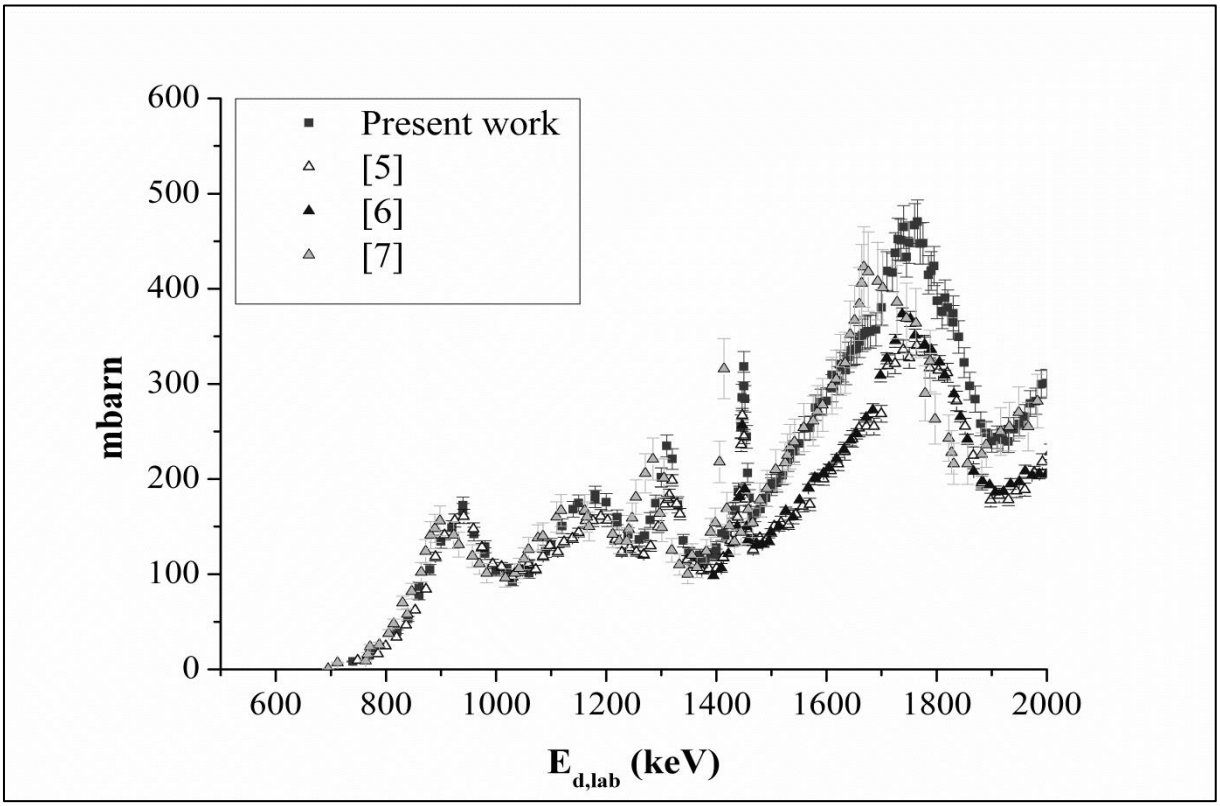
Present work
[5]
[6]
[7]
mbarn
0
100
200
300
400
500
600
600
800
1000
1200
1400
1600
1800
2000
E d,lab (keV)

Table 1.

	Ref. [5]	Ref. [6]	Ref. [7]	Present
Thickness of carbon target (atoms/cm²)	~0.36 x10^{18}*	~2.00x10^{18}*	0.52x10^{18}	1.90 x 10^{18}
Energy loss in target at Ed = 1.45 MeV (keV)	2.1	11.2	2.9	10.5
Target backing	Ta	Ta	Ta	self supp.
Target other	-	Au	-	Pd
Target current (nA)	1000	700	70-130	25
Method of charge collection	not given	Au-RBS	BrookhavenIC	Pd-RBS
Collected charge (μC)	1800	not given	30	7
Target-detector distance (cm)	15	16	7	9.5
Ge det. volume	planar 10 cm^3	planar 10 cm^3	115 cm^3	170 cm^3
Ge det. angle	0	0	135°	55°
Particle detector	no	90° and135°	no	135°
Ed range (MeV)	0.8-2.2	1.4-3.2	0.5-4.0	0.74-2.0
Cross. sect. unit	arbitrary	mbarn	mbarn	mbarn
Uncertainty	not given	12%	10%	6%

*Calculated by us from the energy loss

Fig. 4.

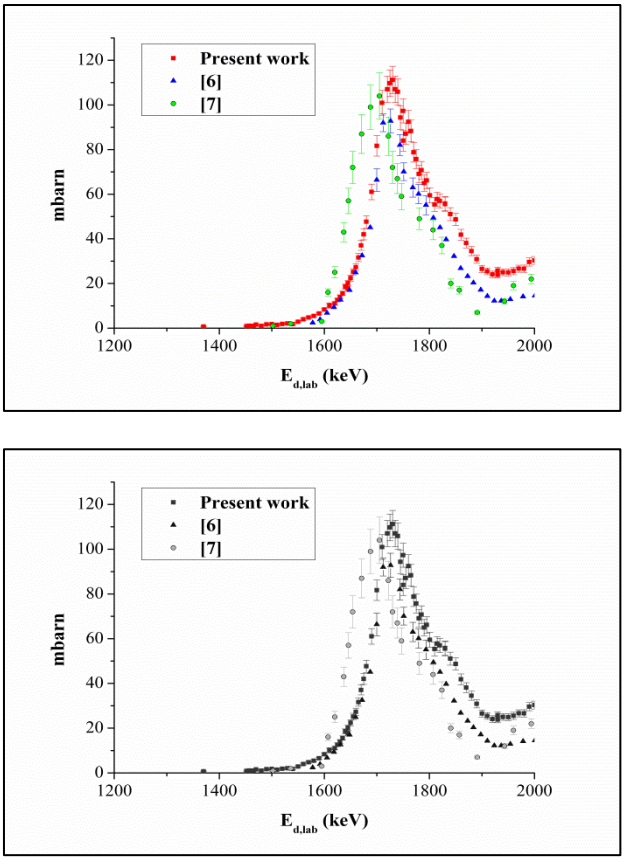
Present work
[6]
[7]
mbarn
$E_{d,lab}$ (keV)

Fig. 5.

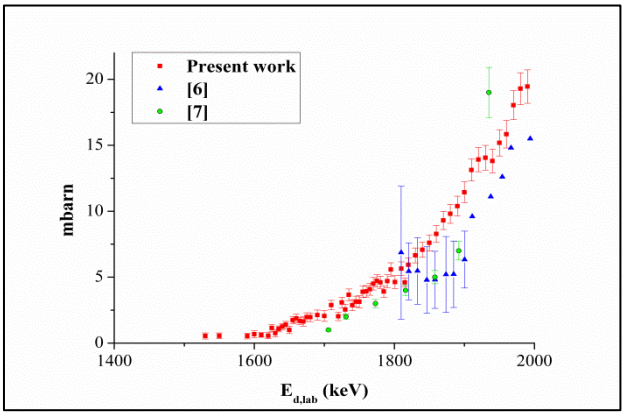
Present work
[6]
[7]
mbarn
$E_{d,lab}$ (keV)

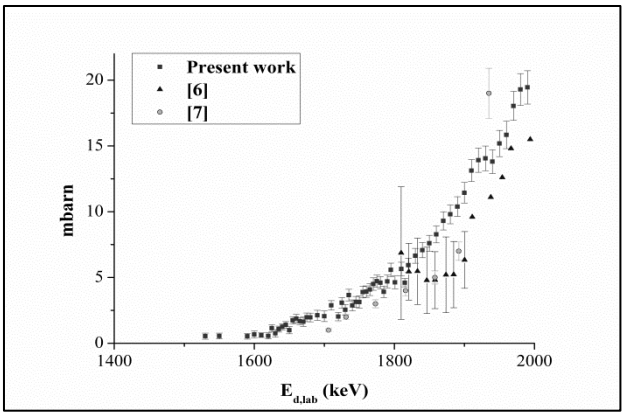

Table 2.

Gamma line keV	Thickness of kapton in μm	Nominal mass fraction of carbon in g/g	Calculated mass fraction of carbon in g/g
3089	125	0.691	0.71±0.04
3684	125	0.691	0.71±0.04
3089	16	0.691	0.72±0.04
3684	16	0.691	0.71±0.04

Fig. 6.

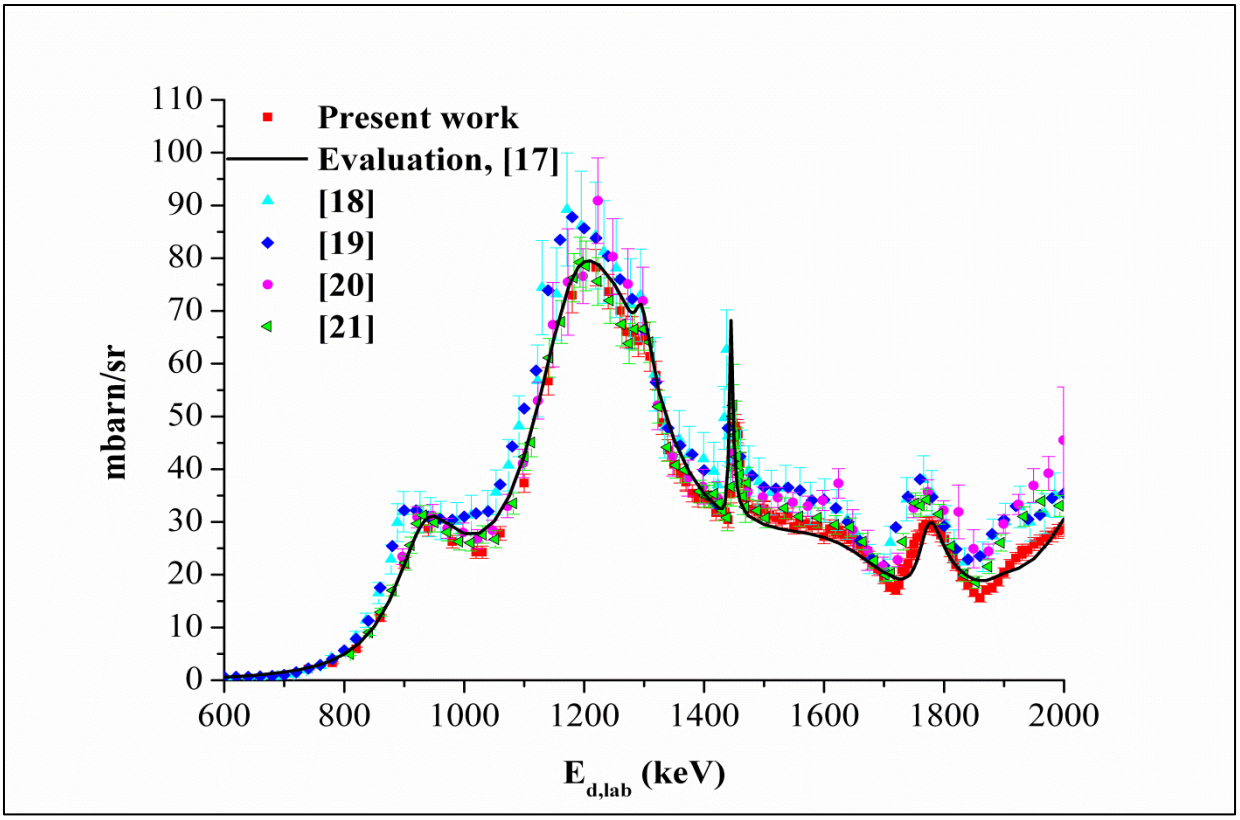
Present work
Evaluation, [17]
[18]
[19]
[20]
[21]
mbarn/sr
E d,lab (keV)

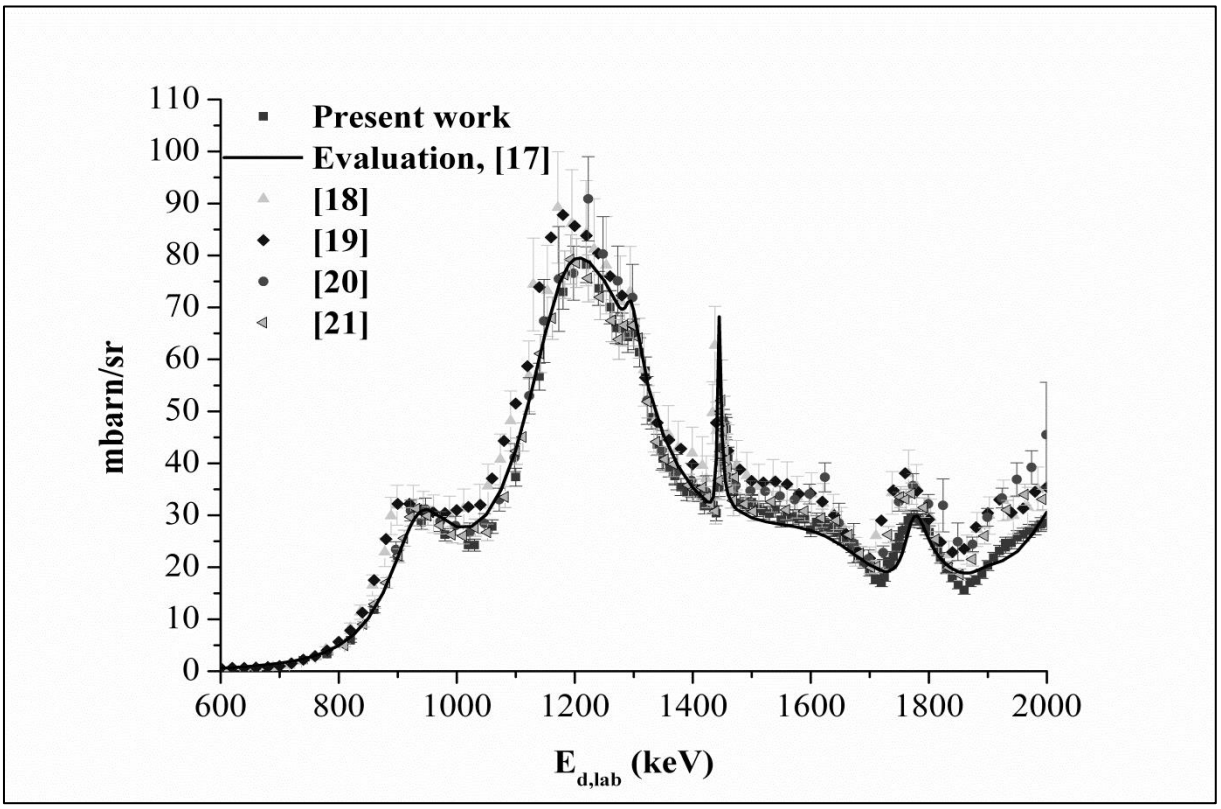
Present work
Evaluation, [17]
[18]
[19]
[20]
[21]
mbarn/sr
E d,lab (keV)

Fig. 7.

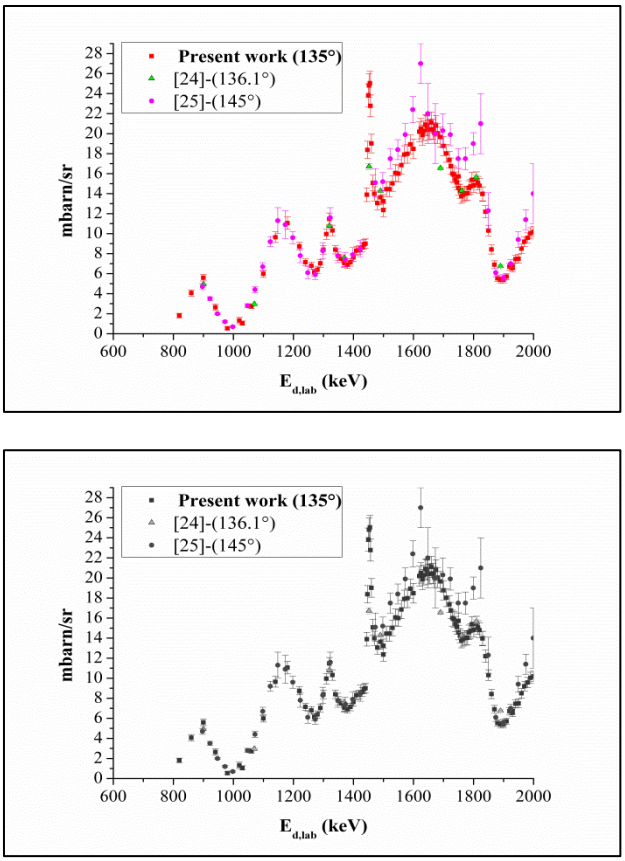
Present work (135°)
[24]-(136.1°)
[25]-(145°)
mbarn/sr
E d,lab (keV)
Present work (135°)
[24]-(136.1°)
[25]-(145°)
mbarn/sr
E d,lab (keV)

Fig. 8.

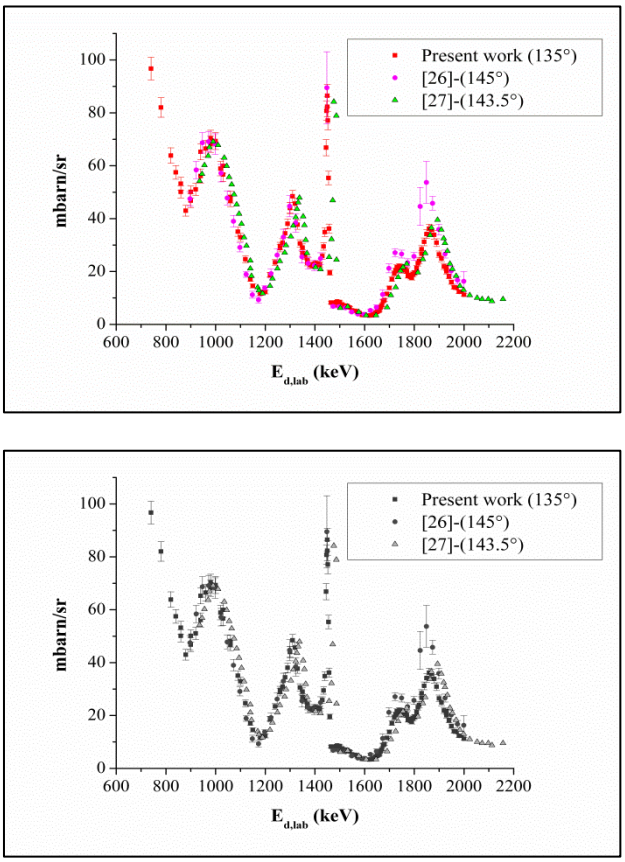
Present work (135°)
[26]-(145°)
[27]-(143.5°)
mbarn/sr
E d,lab (keV)
Present work (135°)
[26]-(145°)
[27]-(143.5°)
mbarn/sr
E d,lab (keV)